

Influence of Machining Process and Machining Induced Surface Roughness on Mechanical Properties of Continuous Fiber Composites

M. Haddad · R. Zitoune · F. Eyma · B. Castanié

Received: 20 June 2014 / Accepted: 3 November 2014 / Published online: 12 November 2014
© Society for Experimental Mechanics 2014

Abstract This paper focuses on the mechanical behavior in quasi-static tests (compression and inter-laminar shear) of two composite materials machined by different processes. First, the impact of the variation of average surface roughness (R_a) and the machining process is studied for both materials and for each stress. The results of compression and inter laminar shear tests show that the mechanical behavior is greatly affected by the surface roughness and the machining temperatures. Secondly the effect of machining processes is detailed. The experimental results show the major dependence of the mechanical behavior on the machining process. The results obtained on the two materials being different, this work sheds light on the influence of the composition of composite materials on the surface defects and the mechanical behavior of such materials.

Keywords Carbon fibers · Mechanical properties · Mechanical testing · Machining temperatures

M. Haddad (✉) · R. Zitoune
Université de Toulouse, INSA, UPS, Mines d'Albi, ISAE, ICA
(Institut Clément Ader), 11UT-A GMP 33 c, Avenue de Rangueil,
31077 Toulouse, France
e-mail: haddad.madjid@gmail.com

F. Eyma
Department of GMP, Université de Toulouse, INSA, UPS, Mines
d'Albi, ISAE, ICA (Institut Clément Ader), IUT de Tarbes 1,
rue Lautreamont, 65000 Tarbes, France

B. Castanié
Université de Toulouse, INSA, UPS, Mines d'Albi, ISAE,
ICA (Institut Clément Ader), INSA, 135 Avenue de Rangueil,
31077 Toulouse, France

Introduction

Composite Fibers Reinforced Polymers (CFRP) are becoming increasingly used in a variety of applications (aerospace, transportation, medical devices...), because of their high (resistance/weight) ratio. Machining is always needed after the demolding of composite parts. This is done in order to achieve the final dimensions and to obtain specific geometrical tolerances. Trimming is the first machining operation and is carried out to remove the matrix overflow from the sides of the composite part. Trimming can be performed using conventional machining (edge trimming, abrasive machining) or non-conventional machining (abrasive water jet). This machining operation is always accompanied by defects [1–7], which are located at the free edges of composite parts (fibers pull-out and/or delamination) or in the thickness (fiber pull-out and resin degradation) [1, 2, 5–8]. These types of damages are influenced by machining conditions, tool geometry, tool wear and fiber orientation [1, 2, 5–14].

The experimental work conducted by Hintze et al. [15] shows that, the length of the delamination increases with increasing cutting edge radius (caused by the tool wear). The augmentation of delamination with increased tool wear is well observed during drilling of composite materials [16–18]. Based on works of [19–21], fiber content and the manufacturing process of the composite part affect also these damages.

Abrasive water jet machining is a non-conventional machining process used in industry for trimming hard materials (inconel, titanium, etc.) and for heterogeneous materials such as composites [24–28]. AWJM offers operators the possibility of avoiding the use of special protection against harmful carbon dust for themselves or the machines [26], as the dust generated is embedded in the water jet and evacuated. The defects generated by abrasive water jet machining are streaks that appear at the exit of the water jet. These streaks increase with the thickness of the plate. Their sizes increase with

increasing distance from the entry of the jet. This increase is strongly connected to the jet pressure, which decreases in the thickness of the machined composite, generating more defects [27].

The average arithmetic roughness R_a remains the qualifying parameter for the surface in composite structures. This criterion widely used in industry and which serves to predict the mechanical behavior of metallic structures, poses a number of problems when trying to extend it to composite materials. In [3, 4], the authors show that this criterion is not adapted to unidirectional specimens oriented at $+15^\circ$, -15° , $+45^\circ$ and -45° made of glass/epoxy composite layers and machined by a cutting tool. For instance, the results of mechanical tensile tests carried out on unidirectional (UD) samples made of glass fibers and epoxy resin and oriented at $+45^\circ$ relative to the axis of loading [3] have shown that the tensile strength increases with the increase in average roughness (R_a). Other authors have found that the (R_a) criterion holds for composite structures. In [15] the authors focused on compression tests on UD oriented at 0° and recorded a decrease of 14 % when the surface roughness R_a increased from 4 to 6 μm , and a decrease of 33 % when the surface roughness varied from 4 to 22 μm . These studies concerned the trimming of a UD oriented at 0° , made of carbon/epoxy composite layers and machined by abrasion.

When comparing different machining processes used on multidirectional CFRP: abrasive water jet (AWJ) machining, cutting with an abrasive diamond cutter (ADS) and edge trimming with polycrystalline diamond (PCD), some authors [22, 23] found that the abrasive diamond cutter provided the best results in terms of roughness and bending mechanical resistance. The PCD specimens gave a good surface roughness (R_a) but led to the poorest bending mechanical resistance. Finally, the bending mechanical resistance of AWJ samples decrease with the increase of the average surface roughness (R_a). It had been shown in a previous work [29], comparing the abrasive water jet machining, ADS machining and conventional tool machining, that the mechanical behavior is strongly affected by the machining process and that AWJM provides better results in quasi static compressive tests while tool machining provides better results in fatigue tests. It is thus clear that the mechanical behavior is affected by the stress mode (quasi-static, fatigue) and the machining process. Other works of [30–33] have also shown the effect of the machining process on the mechanical behavior of composite materials. For example Ramulu and al. [32] showed that abrasive water jet trimming of graphite/epoxy laminates tended to produce exit ply delaminations. However they also found that these delaminations did not significantly reduce the strength of the laminate. Nevertheless, the delaminations that were induced in edge finishing did result in significant reductions in strength. In this paper we will revisit these effects and put shed light on the influence of the composition of composite materials.

To look further to these issues, specimens of two different carbon / epoxy unidirectional composite materials, IMS/977-2 and T700/M21-GC were prepared. In this study we focus on the impact of generated defects by different machining processes during trimming on the mechanical behavior. The same multidirectional stacking sequence was chosen for both composite materials. The specimens were machined by three different cutting processes: abrasive water jet (AWJ), diamond cutter (ADS) and edge trimming. Different machining conditions were chosen during machining by cutting tool and by abrasive water jet. After the machining operation, the surfaces roughness of the specimens was characterized using a roughness tester. To study the influence of surface defects on the mechanical behavior, all specimens were tested under quasi-static tests. Finally to introduce the effect of the nature of loading compressive and inter-laminar shear tests were carried out.

Experimental Procedure

Material Preparation

Carbon-fiber reinforced plastic (CFRP) composite 5.2 mm thick (20 layers) was used for the trimming studies. The CFRP composite was made using unidirectional prepreps, reference T700/M21-GC and IMS/977-2 supplied by the Hexcel Composite Company. The stacking sequence of the laminate was $[90/90/-45/0/45/90/-45/90/45/90]_S$ so as to obtain a multidirectional laminate. Curing was then carried out at 180°C for 120 min during which time the pressure was maintained at 7 bars in an autoclave. The mechanical properties are summarized in Table 1.

Samples Preparation

The specimens were prepared using three cutting processes, abrasive water jet (AWJ), diamond cutter (ADS) and conventional cutting tool machining.

The abrasive water jet machining (AWJM) specimens were prepared by the company “JEDO technologies” company. The abrasive material chosen is the silicon carbide (SiC) and 220 mesh abrasive particles are used. The abrasive flow rate is set at 300 g/min, the nozzle diameter is 0.25 mm, the mixing tube diameter was 0.76 mm, and the jet pressure is set to 3600 bar. Two feed speeds were chosen, 100 mm/min and 500 mm/min, so as to obtain two levels of surface degradation. Five specimens were prepared for each cutting condition and for quasi-static compressive and inter-laminar shear tests.

ADS samples were machined using a saw DIAMFORCE JANTE CONTINUE-D100-AL19-GR 427 saw. Rectified specimens were firstly machined with an ADS cutter, and then 0.5 mm was removed from each side of the sample so

Table 1 Summary of material parameters and experimental details

Composite Material (T700/M21-GC)	Ply thickness: 0.26 mm, Fiber content: $V_f=59\%$ Stacking sequence with respect to the feed direction: [90/90/-45/0/45/90/-45/ 90/45/90]S Glass transition temperature: $T_g=187\text{ }^\circ\text{C}$
Composite material (IMS/977-2)	Ply thickness: 0.26 mm, Fiber content: $V_f=59\%$ Stacking sequence with respect to the feed direction: [90/90/-45/0/45/90/-45/ 90/45/90]S Glass transition temperature : $T_g=212\text{ }^\circ\text{C}$
Tool	Tungsten carbide burr tool Diameter: 6 mm
Standard cutting tool machining conditions	V_f : Feed (mm/min): 125, 250 and 500 N : Spindle speed (m/min): 350, 700 and 1400 a_c : Radial depth of cut (mm): 2
Abrasive Water Jet Machining	Abrasive # 220, diameter d : 67 μm . Nozzle diameter: 0.25 mm Flow rate of abrasive: 300 g/min. V_f (mm/min): 100, 500. Pressure (bar): 3600

as to give a continuous surface. Also, five specimens were prepared for each quasi static mechanical test.

Conventional cutting tool machining experiments were performed using a “DUBUS” 3-axis milling machine with a maximum spindle speed of 75,000 rpm. These experiments were conducted using a full experimental design (3x3) with different cutting conditions (Tab.1). In addition six specimens were prepared, for compressive tests only, with cutting conditions recommended by the tool manufacturer. These conditions are cutting speed of 150 m/min and feed speed of 1000 mm/min.

To ensure consistent values and in order to remove the influence of tool wear, a new tool was used for each experimental condition. To carry out the full experimental design, nine SGS-CCR-20 M 6 mm diameter tungsten carbide burr tools were used. The radial depth of cut is fixed to 2 mm.

Characterization of Surface Defects

The machined surfaces were analyzed using a “Mitutoyo SJ 500” surface roughness tester, with the total measuring length set to 5 mm to avoid overrun.

Mechanical Experiments

Mechanical quasi-static tests were performed on an Instron testing machine. The compressive and inter-laminar shear experiments were conducted according to the standards AFNOR NF T 51-120-3 and AFNOR NF T 57-104

respectively. The experiment design for compressive tests performed with hydraulic grips to avoid slippage is shown in Fig. 1.

During the compressive tests, a high speed camera (FASTCAM-APX RS model 250 K) was used to follow the rupture mechanisms. The acquisition frequency was set to 1000 images/s.

Results and Discussion

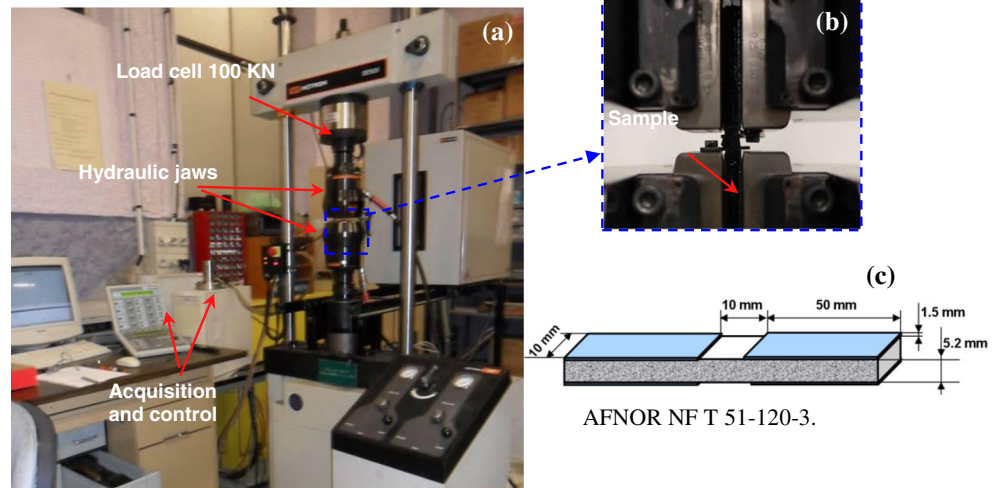
Compression Tests

Fracture mechanisms

Figure 2 plots load versus displacement during compression tests for different machining processes. It is observed that the load increases linearly up to a displacement of 0.2 mm. This increase then becomes non-linear until the first break which corresponds to the maximum load. It can also be noticed that the rupture takes place at three distinct locations (b, c and d). The same curves are obtained for both composite materials (T700/M21-GC and IMS/977-2) regardless of the machining method. High speed camera is used to better analyze the different failure mechanisms.

A high-speed camera (1000 frames per s) was used to better analyze the different failure mechanisms and Fig. 3 shows the images obtained during the compression test performed on a

Fig. 1 Experimental procedure for compressive quasi-static loading. (a) Overview. (b) Zoom on the selected area. (c) Shape of the sample



sample machined by a cutting tool. From these images, it can be seen that the first damage is characterized by the appearance of a crack at the interface ($45^\circ/0^\circ$) corresponding to the fourth and fifth layer of the laminate. This crack was observed when the load reached 11 kN (Fig. 3-a). When the load increases to 12.5 kN a propagation of the crack (probably mode I) throughout the useful part of the specimen was observed (Fig. 3-b). This was accompanied by buckling of the right side of the specimen and a sliding plane in the central area “kink phenomenon” (see Fig. 3-c). At that moment, a sudden load reduction of up to 7 kN is noted. Finally, a slight increase in the load was observed up to 8.2 kN, accompanied by a sudden failure by buckling of the left side of the specimen at the ($0^\circ / 45^\circ$) interface (corresponding to the 16th interface; cf. Fig. 3-d).

The different failure mechanisms observed during the compression test shown above were similar for all specimens and for the different machining processes. This mechanism was

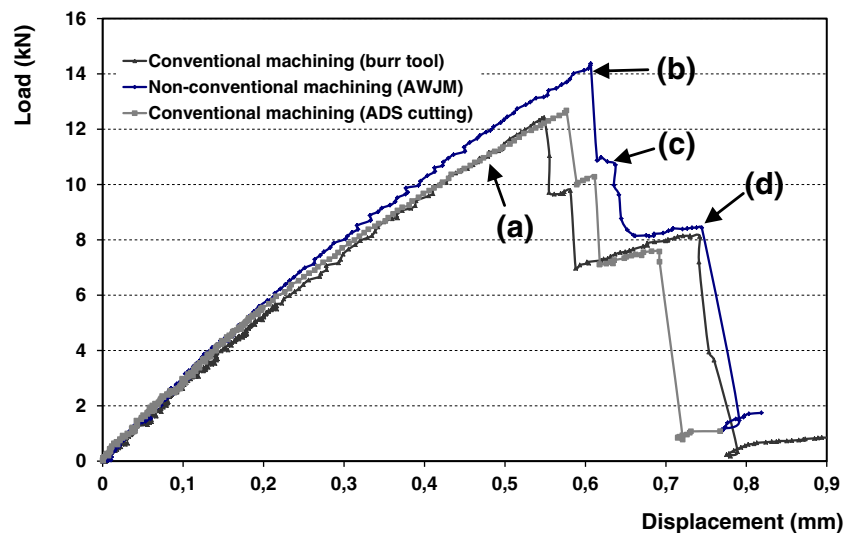
also found to be independent from the quality of the machined surface (R_a) [30–32]. However, the maximum load level recorded was influenced by the machining process on the one hand and by the surface defects (R_a) on the other.

Relationship between compressive strength and machining quality

a) Influence of surface roughness on the stress rupture

Figure 4 shows the evolution of the compressive strength versus the average surface roughness (R_a) for specimens obtained with standard cutting tools. The same behavior was observed for both composite materials (T700/M21-GC and IMS/977-2). An overall reduction of the compressive strength was noted with increases in the surface roughness (R_a). This reduction was 29 % for the composite material T700/M21-GC (34 % for material IMS 977-2) when the surface roughness varies from $4 \mu\text{m}$ (resp. $9 \mu\text{m}$) to $29 \mu\text{m}$ (resp. $47 \mu\text{m}$).

Fig. 2 Evolution of the load versus displacement obtained for compression tests performed on different specimens



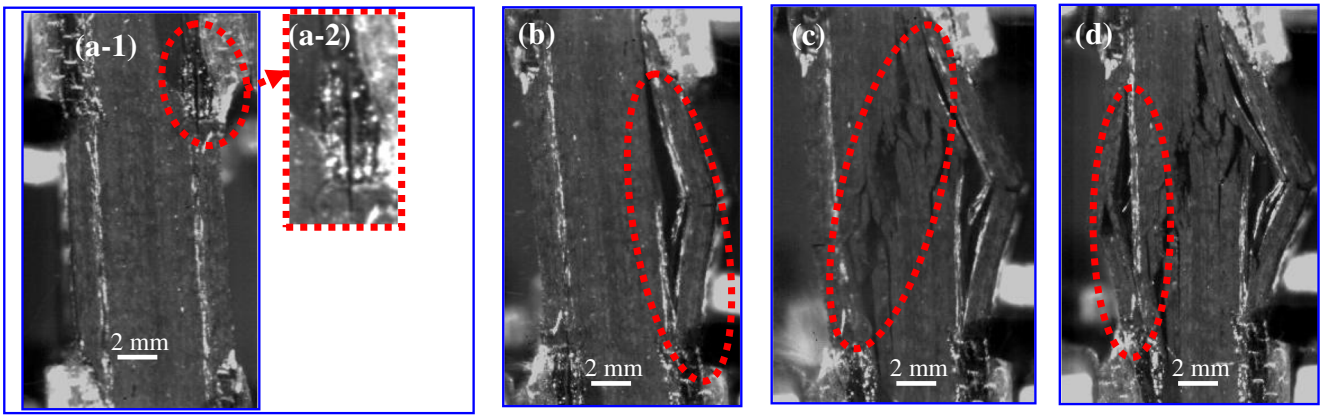


Fig. 3 Images obtained by the high speed camera during the compression test on a specimen machined by cutting tool. (a-1) Appearance of the first crack (11 kN). (a-2) Focus on the area of the appearance of the crack. (b) Propagation of the first crack (first break) (12.5 kN). (c) Appearance of second break: slip plane (9.7 kN). (d) Final Break (8.2 kN)

For the composite material T700/M21-GC, three stages were visible (Fig. 4-a). They can be associated to the machining temperatures. In the first stage, where the compressive strengths were found to be maximum, the machining temperatures (measured by infrared camera) were lower than 130 °C. In the second stage, where the compressive strengths were more stabile and fluctuated around an average value of about 261, the temperatures were between 130 °C and the glass transition temperature (T_g 187 °C). Finally, in the third stage, where a drop in compressive strength was observed, the machining temperatures were higher than the T_g . Similar results were observed for the machining of composite material IMS/977-2 but without the first stage, as the machining temperatures of this composite material are higher than 130 °C.

- b) Influence of machining processes on the rupture stress
- In order to compare the compressive strengths of the specimens resulting from the different cutting processes, samples obtained with a standard cutting tool characterized by surface roughness identical to that of the

specimens obtained with the abrasive water jet and ADS (6.4 μm and 10 μm respectively for the composite material T700/M21-GC, and 9 μm and 11.7 μm for the composite material IMS/977-2) were chosen. The results are shown in Fig. 5. It can be observed that whatever the material machined, the samples obtained by AWJ are characterized by compressive strengths greater than those of specimens machined by the other two processes. For T700/M21-GC specimens having an average surface roughness of 6.4 μm , the differences observed between the compressive strengths of specimens machined by AWJM and those machined by a cutting tool are of the order of 21 %. This difference is around 5 % with respect to ADS cutting. Also, AWJ machining showed low dispersion on the compressive strength (low values of standard deviations) regardless of the material machined. Similar results were obtained on samples from the composite material IMS/977-2. When comparing the sample characterized by a surface roughness of 9 μm , the difference was 29 % between the compressive strengths of specimens machined by AWJM and those machined by

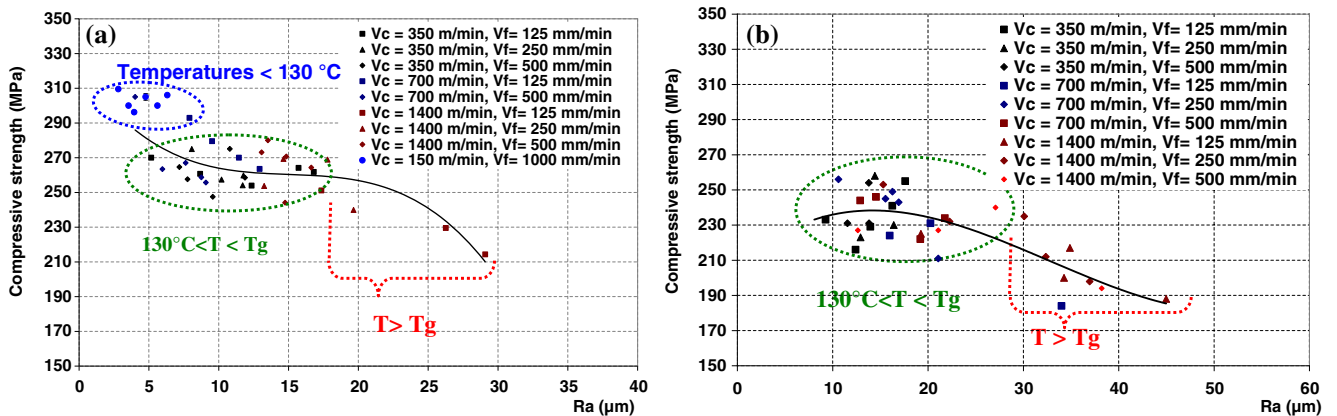
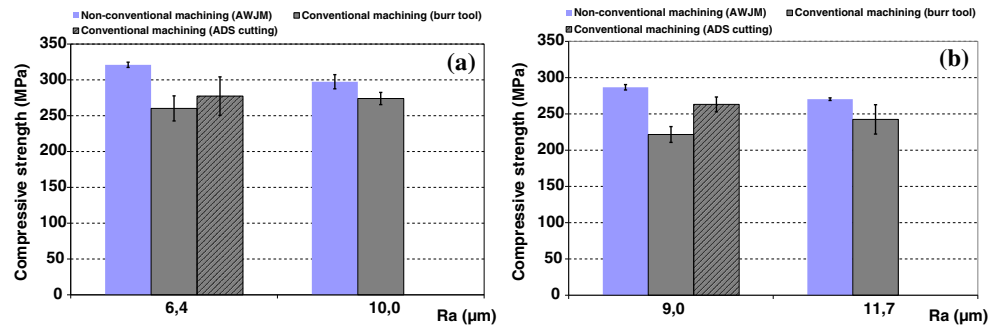


Fig. 4 Compressive strength vs average roughness “Ra” for machining by a burr tool. (a) Composite material T700/M21-GC. (b) Composite material IMS/977-2

Fig. 5 Compressive strength according to average roughness R_a obtained by different machining processes. (a) Composite material T700/M2-GC. (b) Composite material IMS/977-2



a cutting tool. This difference was 23 % when comparing AWJM and ADS machining.

Inter-laminar shear tests

Fracture mechanisms

Figure 6 shows the evolution of the load versus displacement for specimens of the two composite materials (T700/M21-GC and IMS/977-2). The inter laminar shear behavior of all samples is linear elastic with a brittle fracture. It can also be observed that the macroscopic-scale mechanical behavior of the two composite materials studied is very similar.

The fracture appears at the middle of the specimen, slightly to the left or the right of the loading position. Its position corresponds to the eighth interface ($45^\circ/90^\circ$). This crack spreads rapidly and sometimes reaches the edge of the specimen thus forming a through crack. We present a sample obtained by AWJ cutting process below (Fig. 7).

Relationship between inter-laminar shear strength and machining quality

a) Influence of surface roughness on the rupture stress

Figure 8 shows the variation of the inter-laminar shear strength according to the average surface roughness (R_a)

for specimens machined by a burr tool. For composite material T700/M21-GC a small scatter of the results is observed. The general behavior in this case is linear for all the machining temperatures which are between 111°C and 219°C . The inter-laminar shear strength is around 53 MPa and fluctuates between 47 MPa and 58 MPa whatever the surface roughness. Considering the composite material IMS/977-2, an overall reduction in the inter-laminar strengths is noted when the average surface roughness (R_a) increases. Also a considerable scatter can be seen in the inter-laminar shear strength. It is observed that, when temperatures are between 130°C and the glass transition temperature the breaking stresses fluctuate around an average value of 37 MPa, varying between 29 MPa and 46 MPa. However, when machining temperatures are higher than the T_g , a drop in the inter-laminar shear strength is observed. The inter-laminar shear strength fluctuate around an average value of 27 MPa and varies between 23 MPa and 31 MPa. This behavior is similar to that observed in compressive tests for both composite materials T700/M21-GC and IMS/977-2.

The surface roughness of T700/M21-GC was always found to be lower than the surface roughness of IMS/977-2 (Figs. 4, 5 and 8). This may be related to the presence of thermoplastic nodules in the case of the composite material T700/M21-GC (Fig. 9) in addition to the thermoplastic present in the matrix for both composite materials. These

Fig. 6 Load versus displacement obtained for inter-laminar shear tests performed on different specimens. (a) Composite material T700/M21-GC. (b) Composite material IMS/977-2

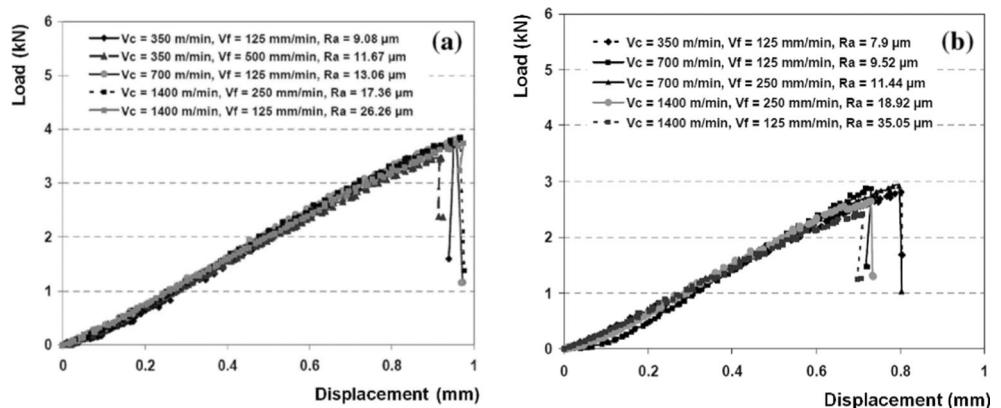
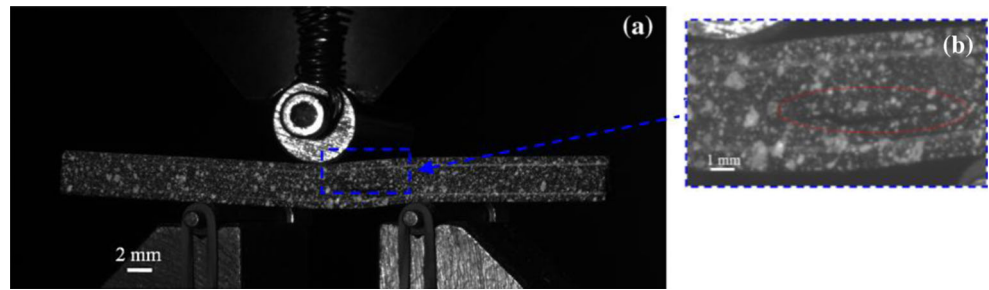


Fig. 7 Apparition of the first crack in inter-laminar shear test on a specimen of T700/M21 GC machined by AWJM obtained with a feed speed of 100 mm/min ($R_a = 6.4 \mu\text{m}$). (a) Overall view. (b) Zoom on the crack region apparition



nodules improve the surface quality of the composite material T700/M21-GC by filling the cracks present on the machined surface. Since these nodules are added to improve the mechanical behaviour of composite materials in term of delamination, they may explain the high resistance of this material in inter laminar shear tests, which promote rupture by delamination whatever the surface roughness (Fig. 8).

Optical observations of the machined surface after trimming with various feed and cutting speeds are presented in Fig. 10 for composite materials T700/M21-GC and IMS/977-2. The presence of different type of damage such as matrix degradation, fiber pull-out and uncut fiber on the free edge of the specimens can be noted in the pictures for both composite materials. Based on these observations, it can be concluded that the maximum damage occurs when machining is done at a high cutting speed (1400 m/min) and low feed speed (125 mm/min). These results confirm the impact of the cutting parameter on the surface roughness. It is also observed that the damages present on the surface of the composite material IMS/977-2 is always more serious and spread over a wider area than that observed on the composite material T700/M21-GC. The presence of high machining temperatures added to the compressive forces directed towards the surfaces of the specimens during the trimming process, cause the thermoplastics to fill the craters observed but also to stick and to

merge with the matrix inside the composite material T700/M21-GC. This phenomenon can explain the difference on the surface damage recorded for the two materials (Fig. 10). Damage is always less in T700/M21-GC than in IMS/977-2, the mechanical behavior is better (less affected by the surface roughness and the machining temperatures) in the case of composite material T700/M21-GC. Thus, thermoplastic nodules improve the machined surface quality and increase the mechanical strength of composite materials.

b) Influence of machining processes on the rupture stress

In order to make a comparison among different specimens obtained by the three cutting processes, samples having the same surface but obtained with a standard cutting tool, an abrasive water jet and ADS ($6.4 \mu\text{m}$ and $10 \mu\text{m}$ for composite material T700/M21-GC and $9 \mu\text{m}$ and $11.7 \mu\text{m}$ for composite material IMS/977-2) were chosen. The results are given in Fig. 11.

For composite material T700/M21-GC (Fig. 11-a), the samples obtained by ADS were characterized by inter-laminar shear strengths greater than those of specimens machined by the other two machining processes. The differences observed between the inter-laminar shear strengths of specimens machined by ADS and those machined by a cutting tool were of the order of 6 %. This difference was around 6.5 % in the comparison with AWJM. For the IMS/977-2 samples (Fig. 11-b), the

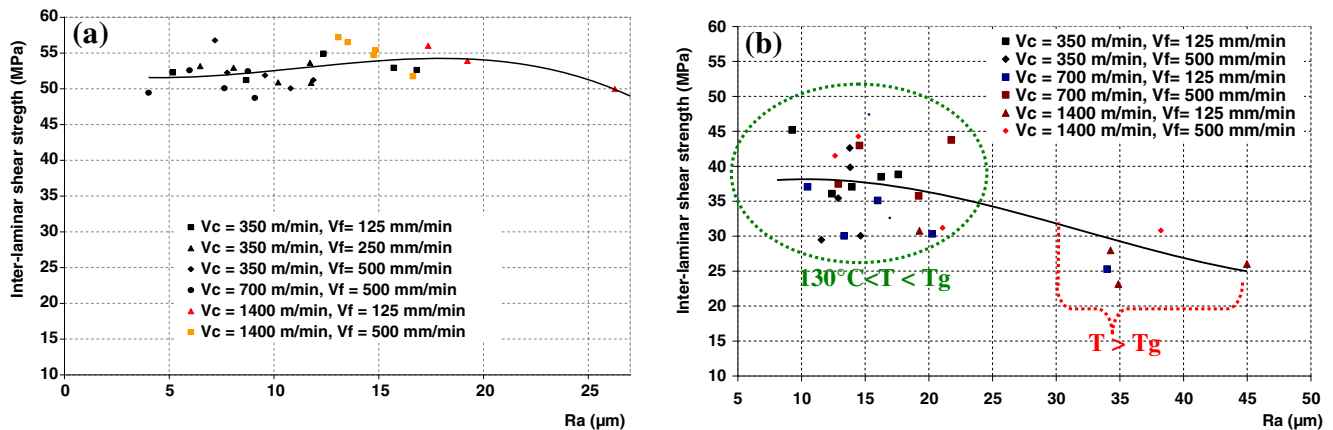
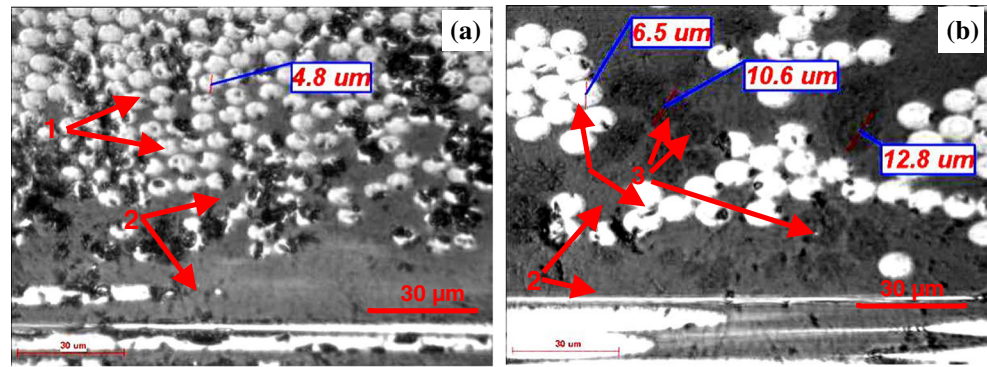


Fig. 8 Inter laminar shear strength vs the average roughness “Ra” when trimming with a burr tool. (a) Composite material T700/M21-GC. (b) Composite material IMS/977-2

Fig. 9 Microscopic images of the machined composite materials. (a) Composite material IMS-977-2. (b) Composite material T700/M21-GC



1- Carbon fibres, 2- Epoxy matrix, 3- Thermoplastic nodules.

results were completely different. In this case, AWJM led to higher inter-laminar shear strengths. For example, when the surface roughness was $9 \mu\text{m}$, the differences were around 29 % between the compressive strengths of specimens machined by AWJM and those machined by a cutting tool (and 11 % between specimens machined by AWJM or ADS).

From these observations it is obvious that the composition of the composite material has a great effect on its mechanical behavior. Depending on the material, a

machining process is suitable for a given stress. In our study, it is clear that abrasive water jet machining is suitable for both materials in the case of compression loads. However, ADS machining is recommended in the case of T700/M21-GC, for better resistance to interlinear shear loading.

This difference can be related to the presence of thermoplastic nodules which improve the mechanical behavior when the machining is performed mechanically (conventional machining). In this case, the machining

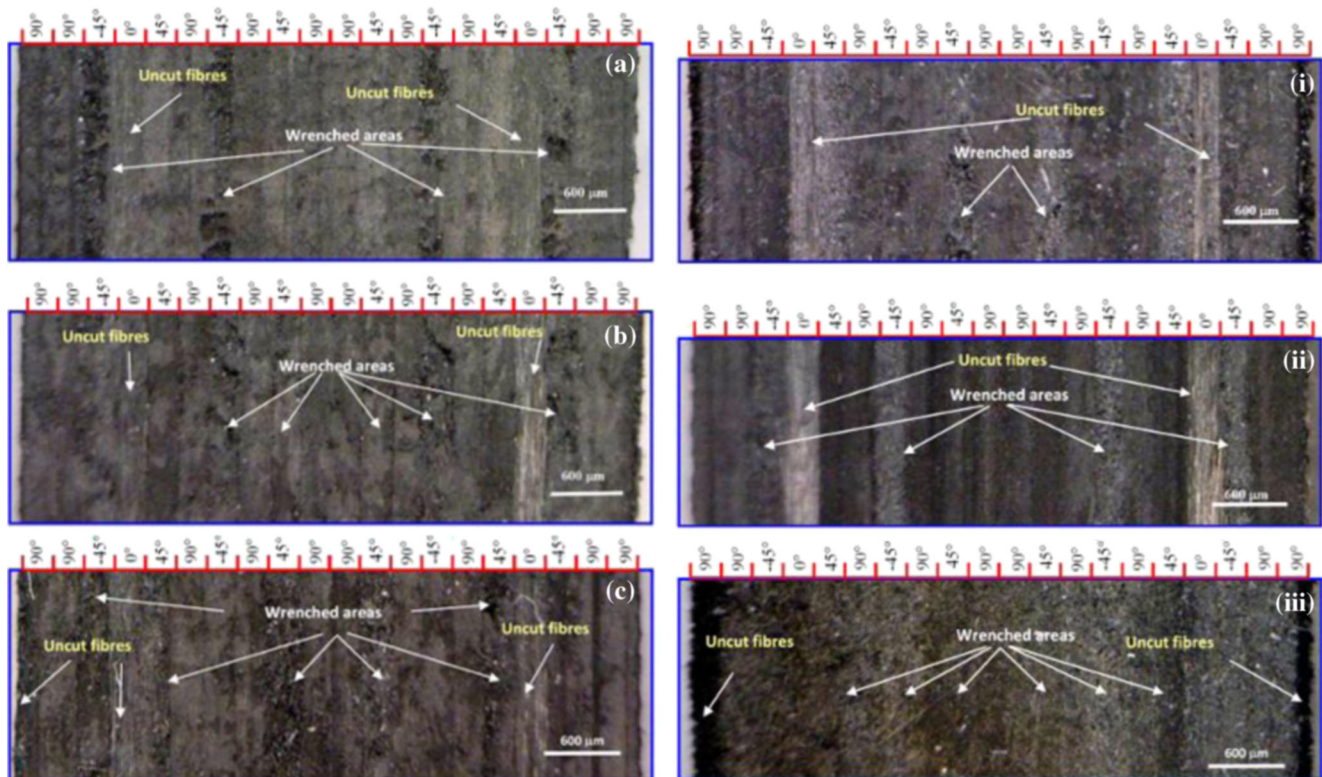
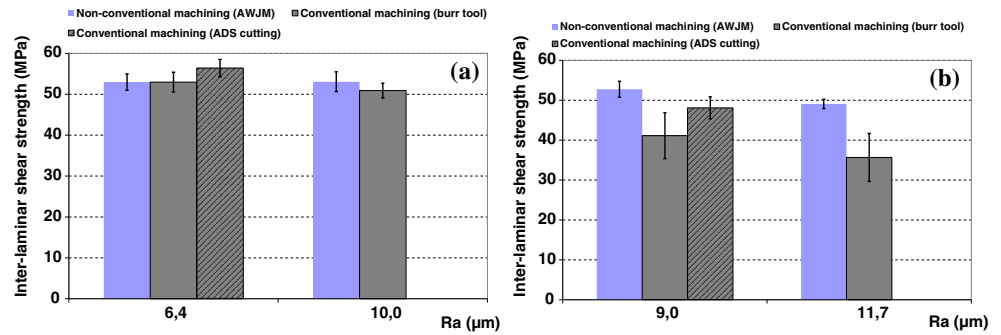


Fig. 10 Optical observations obtained for different machining conditions after a cutting distance of 0.5 m for the composite material T700/M21-GC: (a) $V_c = 700 \text{ m/min}$, $V_f = 500 \text{ mm/min}$, (b) $V_c = 1400 \text{ m/min}$, $V_f = 500 \text{ mm/min}$ and (c) $V_c = 1400 \text{ m/min}$, $V_f = 125 \text{ mm/min}$ and the composite material IMS/977-2: (i) $V_c = 700 \text{ m/min}$, $V_f = 500 \text{ mm/min}$, (ii) $V_c = 1400 \text{ m/min}$, $V_f = 500 \text{ mm/min}$ and (iii) $V_c = 1400 \text{ m/min}$, $V_f = 125 \text{ mm/min}$

Fig. 11 Evolution of inter-laminar shear strength as a function of the average surface roughness R_a obtained by different machining processes. **(a)** Composite material T700/M2-GC. **(b)** Composite material IMS/977-2



temperature combined with the cutting forces help the healing of the machining defects by merging the thermoplastic nodules with the matrix. However, in the case of AWJM, the cutting forces are oriented perpendicular to the machined surface and there are no thermal effects. These facts lead us to think that the thermoplastic nodules make no contribution to the healing of the machined surface, here. In the case of IMS/977-2 there are no thermoplastic nodules and AWJM is again the most suitable machining process.

Conclusions

The main results obtained after the machining and testing of two composite materials having the same stacking sequence under compressive and inter-laminar shear tests are:

- 1 The quality of machined surfaces and the size of the defects generated during machining are strongly influenced by the choice of the machining process, the cutting parameters and also by the component parts of the composite material.
- 2 The quasi-static compressive tests show that the mechanical strength of specimens trimmed by AWJM is greater than the strengths of specimens trimmed by the other two machining processes. Also, a low dispersion on the compressive strength was observed (low standard deviation) for machining by AWJM (demonstrated by the repeatability of the defects all over the specimen [29]).
- 3 The quasi-static inter-laminar shear tests showed that, AWJM machining provided greater inter-laminar shear strengths when the composite material was IMS/977-2 whereas ADS was preferable for T700/M21-GC. This was related to the presence of thermoplastic nodules.
- 4 The mechanical response can be very different from a composite material to another. Therefore, in addition to the machining process and the type of loading, even a slight change in the composition of the composite material

can have a marked effect on the mechanical response. So for each mechanical stress, a different machining process may be more suitable for a given composite material.

Acknowledgements The authors wish to acknowledge the financial support of the French Ministry of research.

References

1. Colligan K, Ramulu M (1991) Delamination in surface plies of graphite/epoxy caused by the edge trimming process. GA, Dec. 1–6, (A93-32021 12–37), p. 113–125. 112th ASME Winter Annual Meeting, Atlanta
2. Guegan P (1994) Contribution à la qualification de l'usinage de matériaux composites à matrice organique. PHD thesis n 2025. Génie Mécanique. E.C. Nantes
3. Ghidossi P, El Mansori M, Pierron F (2004) Edge machining effects on the failure of polymer matrix composite coupons. *Compos Part A* 35(7/8):989–999
4. Ghidossi P, El Mansori M, Pierron F (2005) Influence of specimen preparation by machining on the failure of polymer matrix off-axis tensile coupons. *Compos Sci Technol* 66(11/12):1857–1872
5. Davim JP, Reis P (2005) Damage and dimensional precision on milling carbon fibre-reinforced plastics using design experiments. *J Mater Process Technol* 160(2):160–167
6. Haddad M, Zitoun R, Eyma F, Castanié B (2013) Machinability and surface quality during high speed trimming of multi directional CFRP. *Int J Mach Mach Mater* 13(2/3):289–310
7. Janardhan P, Sheikh-Ahmad JY, Cheraghi H (2006) Edge trimming of CFRP with diamond interlocking tools. *Proceedings of Aerospace Manufacturing and Automated Fastening Conference. ASE* 01(3173): 11–14. Toulouse, France
8. Ahmad JS (2009) *Machining of polymer composites*. Springer, ISBN 978-0-387-35539-9
9. Wang DH, Ramulu M, Arola D (1995) Orthogonal cutting mechanisms of graphite/ epoxy. Part I: unidirectional laminate. *Int J Mach Tools Manuf* 35(12):1623–1638
10. Wang DH, Ramulu M, Arola D (1995) Orthogonal cutting mechanisms of graphite/ epoxy. Part II: multi-directional laminate. *Int J Mach Tools Manuf* 35(12):1639–1648
11. Caprino G, Santo L, Nele L (1998) Interpretation of size effect in orthogonal machining of composite materials. Part I: unidirectional glass-fibre-reinforced plastics. *Compos Part A* 29(8): 893–897
12. Wang XM, Zhang LC (2003) An experimental investigation into the orthogonal cutting of unidirectional fibre reinforced plastics. *Int J Mach Tools Manuf* 43(10):1015–1022

13. Kalla D, Sheikh-Ahmad JY, Twomey J (2010) Prediction of cutting forces in helical end milling fibre reinforced polymers. *Int J Mach Tools Manuf* 50(10):882–891
14. Hintze W, Hartmann D, Schütte C (2011) Occurrence and propagation of delamination during the machining of carbon fibre reinforced plastics (CFRPs)—an experimental study. *Compos Sci Technol* 71(15):1719–1726
15. Zitoun R, Krishnaraj V, Almabouacif BS, Collombet F, Sima M, Jolin A (2011) Influence of machining parameters and new nano-coated tool on drilling performance of CFRP/Aluminium sandwich. *Compos Part B* 44(3):1480–1488
16. Davim JP, Reis P (2003) Study of delamination in drilling carbon fibre reinforced plastics (CFRP) using design experiments. *Compos Struct* 59(4):481–487
17. Shyha I, Soo SL, Aspinwall D, Bradley S (2010) Effect of laminate configuration and feed rate on cutting performance when drilling holes in carbon fibre reinforced plastic composites. *J Mater Process Technol* 210(8):1023–1034
18. Kim D, Ramulu M, Doan X (2005) Influence of consolidation process on the drilling performance and machinability of PIXA-M and PEEK thermoplastic composites. *J Thermoplast Compos Mater* 18(3):195–217
19. El-Sonbaty I, Khashaba UA, Machaly T (2004) Factors affecting the machinability of GFR/epoxy composites. *Compos Struct* 63(3/4):329–338
20. Zitoun R, Collombet F, Guillermo Hernáiz L (2008) Experimental and analytical study of the influence of HexFit glass fibre composite manufacturing process on delamination during drilling. *IJMMM* 3(3/4):326–342
21. Arola D, Ramulu M (1997) Net shape manufacturing and the performance of polymer composites under dynamic loads. *Exp Mech* 37(4):379–385
22. Arola D, Ramulu M (1998) Net shape machining and the process-dependence failure of Fibre reinforced plastics under static loads. *Exp Mech* 20(4):210–220
23. Chen F, Siores E (2001) The effect of cutting jet variation on striation formation in abrasive water jet cutting. *Int J Mach Tools Manuf* 10(41):1479–1486
24. Ferrendier S (2001) Influence de l'évolution granulométrique des abrasifs sur l'enlèvement de matière lors de la découpe par jet d'eau abrasif. PHD thesis, école nationale supérieure d'arts et métiers
25. Hocheng H (1989) A failure analysis of water jet drilling in composite laminates. *Int J Mach Tools Manuf* 30(3):423–429
26. Haddad M, Zitoun R, Eyma F, Castanié B (2014) Study of the surface defects and dust generated during trimming of CFRP: influence of tool geometry, machining parameters and cutting speed range. *Compos Part A* 66:142–154
27. Ramulu M, Jenkins MG, Guo Z (2001) Abrasive water jet machining mechanisms in continuous-fibre ceramic composites. *J Compos Technol Res* 23(2):82–91
28. Wang J (1999) Abrasive water jet machining of polymer matrix composites—cutting performance, erosive process and predictive models. *Int J Adv Manuf Technol* 15(10):757–768
29. Haddad M, Zitoun R, Bougherara H, Eyma F, Castanié B (2014) Study of trimming damages of CFRP structures in function of the machining processes and their impact on the mechanical behavior. *Compos Part B* 57:136–143
30. Colligan K, Ramulu M, Arola D (1993) Investigation of edge quality and ply delamination in abrasive waterjet machining of graphite/epoxy. *Mach Adv Compos ASME ASME Publ N Y* 66:167–186
31. Arola D, Ramulu M (1994) Machining induced surface texture effects on the flexural properties of graphite/epoxy laminates. *Composites* 25(8):822–834
32. Ramulu M, Colligan K (2005) Edge finishing and delamination effects induced during abrasive waterjet machining on the compression strength of a graphite/epoxy composite. Paper Imece2005-82346, Proceedings Of Imece: ASME International Mechanical Engineering Congress & Exposition November 5–11, 2005, Orlando, Florida
33. Briggs TM, Ramulu M (2010) Effect of AWJ machining processes on flexural properties of CFRP composites. TMS Proceedings (CD) on Manufacturing Processes, Feb 15–18th, 2010, Seattle